JMEPEG (2011) 20:706–711
DOI: 10.1007/s11665-011-9831-5

1059-9495/$19.00

Theoretical and Experimental Investigation on SMA Superelastic Springs

Gabriele Attanasi, Ferdinando Auricchio, and Marco Urbano

(Submitted May 9, 2010; in revised form October 11, 2010)

The mechanical behavior of superelastic springs is investigated in this study. The goal is to evaluate the device response and to exploit the material superelastic behavior, main concerns being material and geometrical response nonlinearity. The investigation is made of two parts, i.e., an experimental campaign and a numerical model proposal. Experimental tests have been performed on superelastic SMA coil springs considering load history in tension and compression for three different spring geometrical configurations. Tested specimens experience a maximum elongation larger than the original spring axis length. The response is not symmetric and under compression it is affected by buckling instability. Nevertheless, experimental results show a very good superelastic behavior with no damage and with negligible residual displacements. Numerical analyses have been performed to reproduce the experimental campaign results. A simple finite element model is proposed. Experimental and numerical result agreement is very good. The numerical model turns out to be a powerful design tool even for the very complex geometrical and material nonlinear conditions under investigation. Hence, it is proposed as a useful tool for spring design validation and response prediction.

Keywords experimental test, shape memory alloys, springs

1. Introduction

A mechanical spring may be defined as an elastic body whose primary function is to deflect, distort, or absorb energy under load, able at the same time to recover its original shape when released after being distorted. This definition underlines the fact that springs have been historically designed to accommodate displacements, to provide energy dissipation, restraining, and re-centering force as reported in Ref 1. Moreover, conventional springs are characterized by design displacement values and stresses which are not beyond the elastic limit, so the large majority of springs are designed considering a linear elastic load-displacement response. The goal of this study is to evaluate the response of superelastic springs, i.e., the response of springs made with shape memory alloys (SMA), and exploiting the material superelastic behavior. This means to consider devices designed to work in a nonlinear geometric and material response range, i.e., taking advantage of the nonlinearity, but without renouncing to the recentering and restraining properties. The motivation is the feasibility investigation on the use of superelastic springs as lateral restrainer for applications in which the presence of restoring force is a critical element when the linear limit is exceeded (as proposed in Ref 2 and 3).

This article is an invited paper selected from presentations at Shape Memory and Superelastic Technologies 2010, held May 16–20, 2010, in Pacific Grove, California, and has been expanded from the original presentation.

Gabriele Attanasi, Eucentre, European Centre for Training and Research in Earthquake Engineering, Pavia, Italy; **Ferdinando Auricchio**, Dipartimento di Meccanica Strutturale, Università degli Studi di Pavia, Pavia, Italy; and **Marco Urbano**, Saes Getters, Lainate, Milano, Italy. Contact e-mails: gabriele.attanasi@unipv.it, auricchio@unipv.it, and Marco_urbano@saes-group.com.

2. Review of Shape Memory Alloys Main Properties

Shape memory alloy (SMA) is a functional material with increasing applications in many areas. SMAs have demonstrated energy dissipation capabilities, large elastic strain capacity, hysteretic damping, good high and low-cycle fatigue resistance, recentering capabilities and excellent corrosion resistance. An exhaustive description of SMA properties, potentials, and current applications is provided by Song et al. (Ref 4), Desroches and Smith (Ref 5), and Wilson and Wesolowsky (Ref 6). The most important properties showed by the SMA are the shape memory and the superelastic effects. These unique properties are the result of reversible phase transformations. There are two crystal structure phases in SMAs: the austenite, stable at high temperature, and the martensite, stable at low temperature (see Ref 7). In its low temperature phase, if loaded, SMAs exhibit the shape memory effect (SME). When SMAs in martensite are subjected to external stress, they deform through the so-called detwining mechanism up to several percent strains. Unloading results in a residual strain, as shown in Fig. 1. Heating the previously deformed specimen above a determined temperature results in phase transformation, and a recovering of the original shape (removal of the residual strain, see Ref 6). In its high temperature form, SMAs exhibit a superelastic effect. Originally in austenitic phase, martensite is formed upon loading

beyond a certain stress level, resulting in the stress plateau shown in Fig. 2. However, upon unloading, the martensite becomes unstable, resulting in a transformation back to austenite and the recovery of the original, undeformed shape (see Ref 6).

3. Superelastic Coil Spring Experimental Tests

Experimental tests have been performed on superelastic material coil springs produced by SAES Getters (www.saesgetters.com), a shape memory alloy world company.

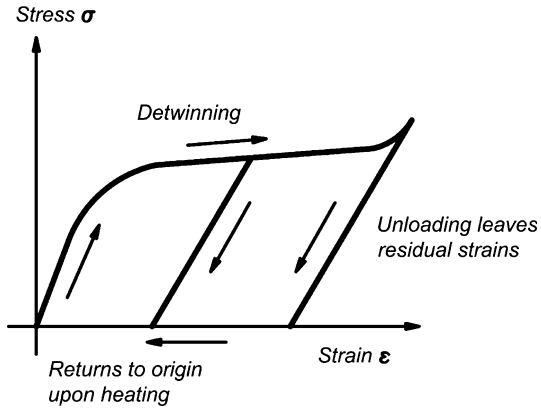

Fig. 1 Idealized stress-strain curve for shape memory effect

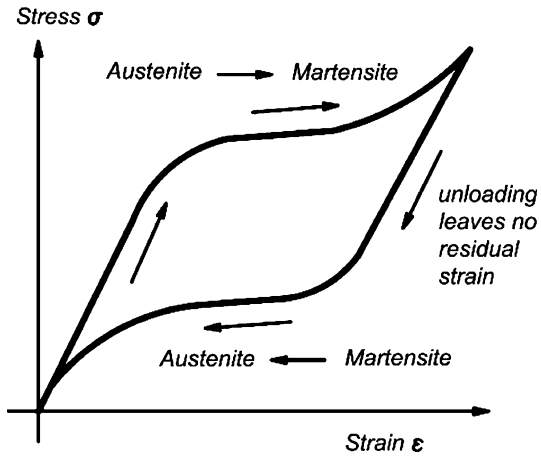

Fig. 2 Idealized stress-strain curve for superelastic effect

3.1 Experimental Specimens Geometry

Tested specimens are characterized by the following geometry: the coil is made of a 1 mm diameter superelastic shape memory alloy wire. It has been hot formed, being winded on a circular bar of 5 mm radius under tension. The coil height is about 7.5 mm. Three specimen configurations have been manufactured and are shown in Fig. 3, respectively, with 3 coils (S1A, in Fig. 3a), 4 coils (S2A, in Fig. 3b), and 5 coils (S3A, in Fig. 3c).

3.2 Experimental Set Up

For the uniaxial test in tension and in compression, a universal testing machine was used. The clamping system solution has been an issue in the experimental tests campaign. Due to the particular material and to the dimension of the coil wire, it has not been possible to weld the spring dead coil to a particular clamping system. The used solution is shown in Fig. 4. It consists of an Allen screw whose head diameter is the same as the winding bar diameter. The coils fit around it and the dead coil is fastened using a bolt and a little steel plate inserted in the screw as well. The screw has then been fastened to the clamping pliers of the testing machine. The test environment temperature was 22 °C.

3.3 Results of Experimental Testing

The different protocols and results of tension-compression axial tests on the springs are described in this section. Tested specimens were new samples, never having experienced any displacement history before being tested. Nevertheless, some of them being tested two times, they have shown the same skeleton curve, without any damage-induced difference.

Since the tested specimens are slender, an important issue affecting spring response in compression is buckling. Thus, the spring maximum compression load is related to fly out instability phenomena more than theoretical compression

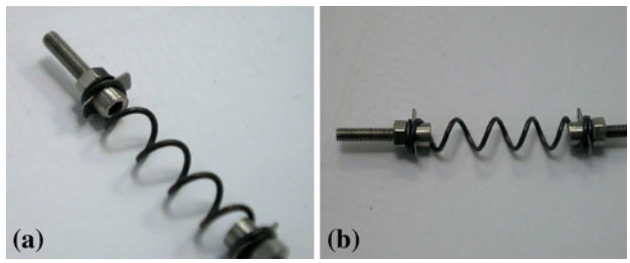

Fig. 4 Spring clamping system solution. Views 1 (a) and 2 (b)

Fig. 3 Tested superelastic spring specimens. (a) S1A (b) S2A (c) S3A

capacity. Moreover, from the results it turned out that the clamping system influenced the tests. This is due to the contact between the coil wire and the head of the Allen screw. In tension, the Allen screw head being of the same diameter of the internal coil diameter when the spring is not loaded, it prevents the reduction of diameter of the coil providing more stiffness and reducing the expected displacement for the same level of force. In compression, the influence is even more important because it limits significantly the maximum displacement capability of the spring before reaching the contact between the elements and further affects the buckling load in the member. Nevertheless, results turned out to be very interesting, regardless of the few problems related to the boundary conditions.

3.3.1 Specimen S1A. The specimen S1A is the 3 coils spring, the total axis length is about $h_{S1A} = 22.87$ mm (as shown in Fig. 3a). Two displacement controlled tests have been performed on the spring, considering the following displacement histories:

- test #1: 0 mm, +4 mm, −4 mm, +8 mm, −8 mm, +12 mm, −12 mm, 0 mm
- test #2: 0 mm, +15 mm, −10 mm, +20 mm, −10 mm, +25 mm, −10 mm, +30 mm.

Tests were performed waiting few hours from the first test before performing the second one. The response curve is exactly the same showing no difference between the "virgin" sample and the "tested" sample response.

Maximum displacement in compression Δ_{cS1A} and in tension Δ_{tS1A} over the spring axis length ratios are, respectively, $\Delta_{cS1A}/h_{S1A} = 52\%$ $\Delta_{tS1A}/h_{S1A} = 131\%$. Limitation in compression displacement is due to boundary condition geometry compatibility. The test velocity was constant and equal to 4 mm/min. Two snapshots of the deformed spring during the test are shown in Fig. 5. Results of the performed tests are shown in Fig. 6. Data report a quite stable global superelastic response of the axially loaded spring. Some irregularities in the response curve are shown in correspondence of large positive displacements. These are due to the contact phenomena between the coil wire and the clamping system. After the test, the specimen has been checked and measured. The spring wire resulted undamaged and the initial geometry was perfectly recovered.

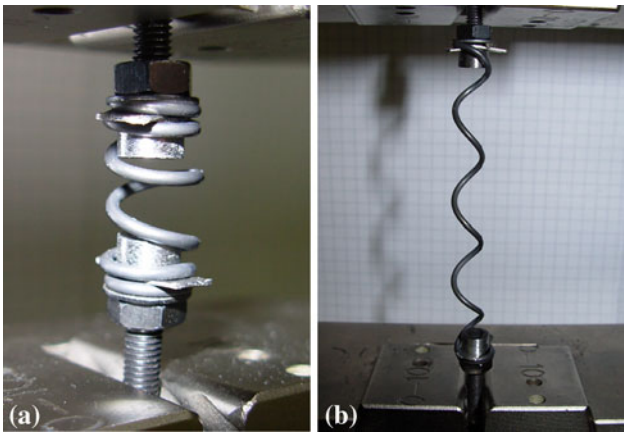

Fig. 5 Specimen S1A experimental test pictures. (a) Maximum compression (−15 mm) and (b) maximum tension (+30 mm)

3.3.2 Specimen S2A. The specimen S2A is the 4 coils spring, the total axis length is about $h_{S2A} = 27.61$ mm (as shown in Fig. 3b). Two displacement controlled tests have been performed on the spring, considering the following displacement histories:

- test #1: 0 mm, +10 mm, −10 mm, +15 mm, −15 mm, +20 mm, −20 mm, 0 mm
- test #2: 0 mm, +25 mm, −10 mm, +30 mm, −10 mm, +35 mm, −10 mm, +40 mm, 0 mm.

Again, no differences in response between the "virgin" sample and the "tested" sample response were recorded. Maximum displacement in compression Δ_{cS2A} and in tension Δ_{tS2A} over the spring axis length ratios are, respectively, $\Delta_{cS2A}/h_{S2A} = 72\%$ $\Delta_{tS2A}/h_{S2A} = 145\%$. Limitation in compression displacement is due to boundary condition geometry compatibility. The test velocity was constant and equal to 4 mm/min. Two snapshots of the deformed spring during the test are shown in Fig. 7. Results of the performed tests are shown in Fig. 8. During the maximum compression displacement, lateral buckling and contact between the coil wire and the clamping system was reached as shown in Fig. 7(a), and this led to maximum compression force peak. However, the spring system is

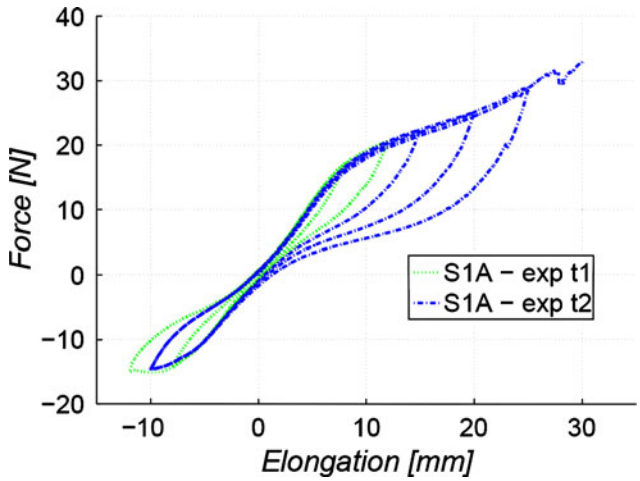

Fig. 6 Specimen S1A experimental test results

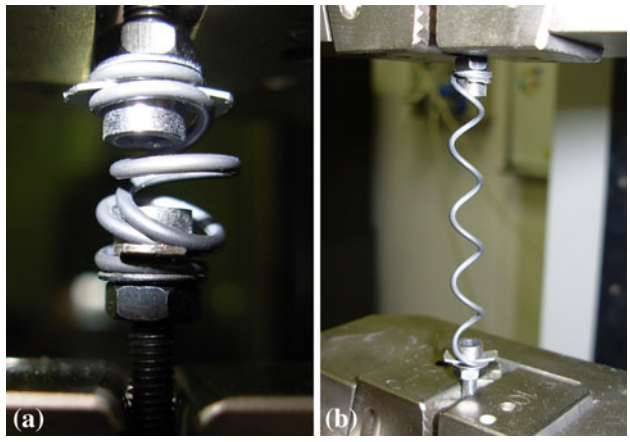

Fig. 7 Specimen S2A experimental test pictures. (a) Maximum compression (−20 mm) and (b) maximum tension (+40 mm)

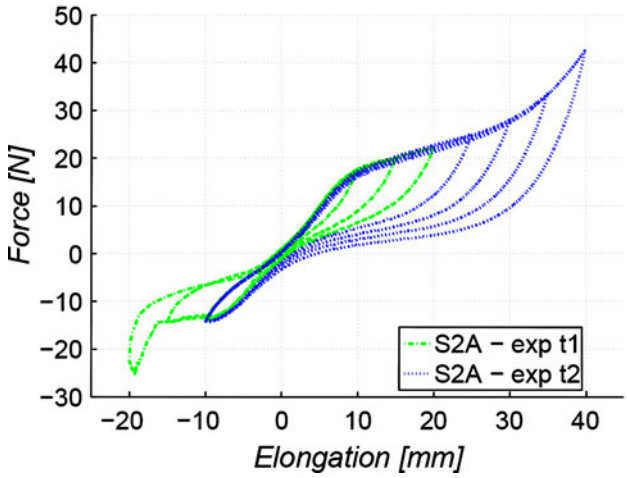

Fig. 8 Specimen S2A experimental test results

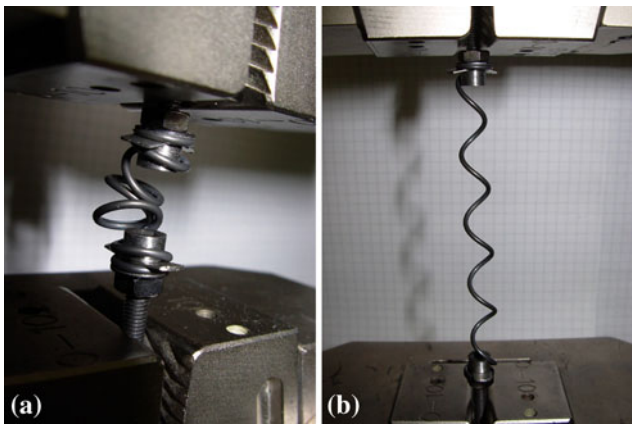

Fig. 9 Specimen S3A experimental test pictures. (a) Maximum compression (−15 mm) and (b) maximum tension (+40 mm)

characterized by a very good and stable flag-shaped response. Again the specimen shows a perfect superelastic behavior. After the test, the spring wire resulted undamaged and the initial geometry was perfectly recovered.

3.3.3 Specimen S3A. The specimen S3A is the 5 coils spring, the total axis length is about $h_{S3A} = 35.07$ mm (as shown in Fig. 3c). A displacement controlled test has been performed on the spring, considering the following displacement history:

- test #1: 0 mm, +10 mm, −10 mm, +20 mm, −10 mm, +40 mm, −15 mm, 0 mm.

Maximum displacement in compression Δ_{cS3A} and in tension Δ_{tS3A} over the spring axis length ratios are, respectively, $\Delta_{cS3A}/h_{S3A} = 43\%$ $\Delta_{tS3A}/h_{S3A} = 114\%$. Limitation in compression displacement is due to boundary condition geometry compatibility. The test velocity was constant and equal to 4 mm/min. Two snapshots of the deformed spring during the test are shown in Fig. 9 and it is shown lateral buckling in compression. Results of the performed tests are shown in Fig. 10. The spring system is characterized by a very good and stable flag-shaped response and the specimen shows a perfect superelastic behavior, without residual deformations or damages.

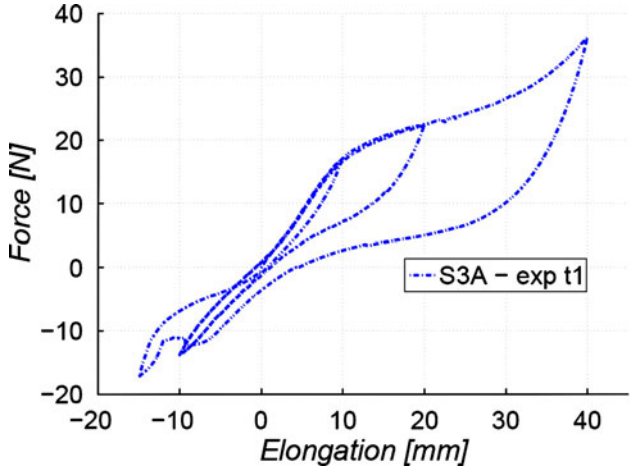

Fig. 10 Specimen S3A experimental test results

4. Numerical Simulations

Numerical simulations have been performed to reproduce the response of the same specimens tested in the experimental campaign. The philosophy followed in the modelling is to use a model as simple as possible. For this reason, the spring has been modelled using two-node simple beam elements reproducing the wire axis geometry. Since the elements are straight, each single coil has been approximated using 36 elements. The circular section has been assigned. Regarding the boundary conditions, even if the clamping system is quite complex to be described, fixed conditions for both the end nodes are applied. The superelastic material model defined in the commercial finite element (FE) code ABAQUS (see Ref 8) has been considered and the material properties have been identified as reported in the following section.

4.1 Material Characterization

To manufacture the spring, the original wire is subjected to thermo-mechanical treatments which alter the original properties. Hence, it is not possible to perform tests on the original wire to detect the material properties. For this reason, the experimental results relative to specimen S1A are used to compute material properties through a trial and error fitting process. Accordingly, several numerical analyses were performed considering the given geometry, changing between different material properties until the model has been able to describe in a suitable way this single test results. Then, the final parameters have been used to predict the results of specimens S2A and S3A. Since they have been found independently from these results, this is a correct validation process. Referring to the model shown in Fig. 11 and defined in Ref 8, the material parameters are reported in Table 1.

The corresponding material, considering a simple uniaxial tension test using a FE analysis program (Ref 8), shows the behavior reported in Fig. 12. No temperature dependence has been considered in the material properties.

4.2 Numerical and Experimental Testing Result Comparison

A very simple model has been used to predict the response of superelastic coil springs tested and results are very good. There are some differences between the real response and the

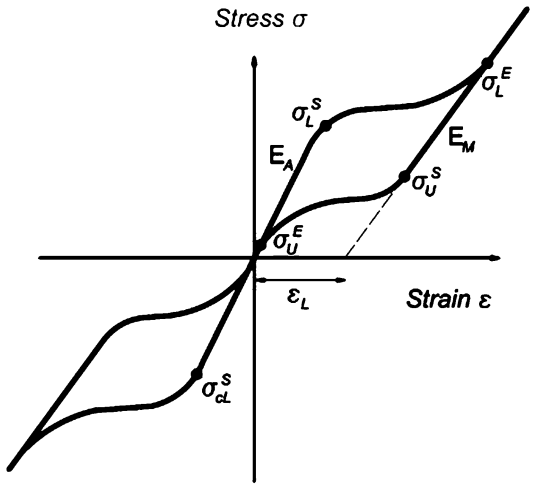

Fig. 11 SMA superelastic stress strain relation (from Ref 8)

Table 1 SMA superelastic material properties

E_A = 32000 MPa	σ_L^S = 350 MPa	σ_U^E = 10 MPa
E_M = 12000 MPa	σ_L^E = 375 MPa	σ_{cL}^S = 350 MPa
$\nu_A = \nu_M$ = 0.33	σ_U^S = 200 MPa	ε^L = 7%

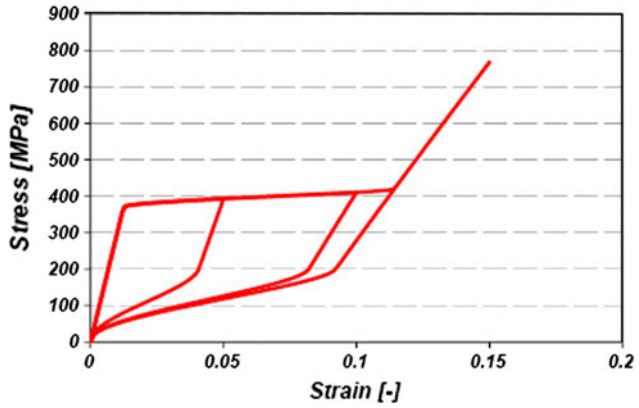

Fig. 12 SMA constitutive relation for the considered specimen

FE model results, but they can be considered negligible and the numerical analysis is able to predict all the main experimental data in terms of force-displacement relation.

4.2.1 Specimen S1A. Comparison between experimental and numerical test result for specimen S1A is shown in Fig. 13. The numerical model is describing very well the experimental test results. Of course it is not affected by instability due to clamping system contact effect on the coil wire, but beside this, the experimental response is very well modelled. In tension, the initial elastic stiffness, the loading cycle, and the unloading cycle resulting from FE analysis are very close to the experimental data. In compression the FE analysis underestimates the unloading stiffness. Moreover it predicts a buckling which is not occurring in the experiments. Probably this is due to the fact that the model does not take into account the clamping system effectiveness in reducing the free length of the spring and in conditioning the displacement capability of the coil wire.

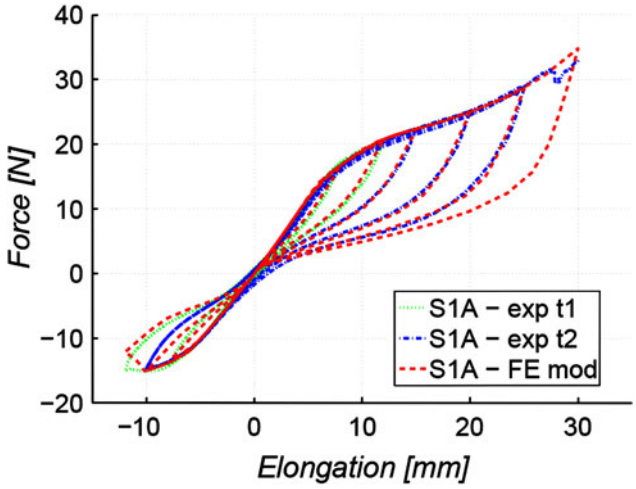

Fig. 13 Specimen S1A experimental and numerical test result comparison

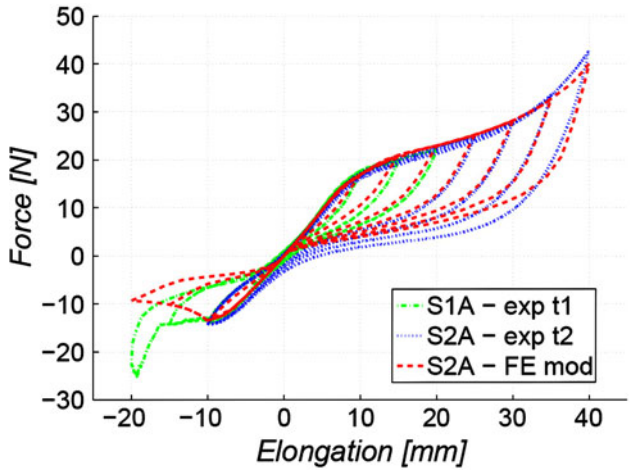

Fig. 14 Specimen S2A experimental and numerical test result comparison

4.2.2 Specimen S2A. Comparison between experiments and numerical test result for specimen S2A is shown in Fig. 14. In compression, numerical results overestimate the buckling, while they do not consider the contact problem due to the clamping system. This is due to the incapacity of the adopted simple model to describe this phenomenon. In tension response, for low-displacement cycles the unloading stiffness is a bit underestimated, as well as the maximum force and the residual displacement at the end of each large-displacement cycle. Anyway, due to the fact that differences are very small, numerical result reproduces very well the specimen force-displacement behavior.

4.2.3 Specimen S3A. Comparison between experimental and numerical test result for specimen S3A is shown in Fig. 15. Again, the FE model can be considered quite well in predicting the experimental response. The instability in compression is not captured perfectly, the maximum force is slightly overestimated, and the residuals are slightly underestimated. Nevertheless elastic limit and after yielding behavior are well described both in tension and in compression.

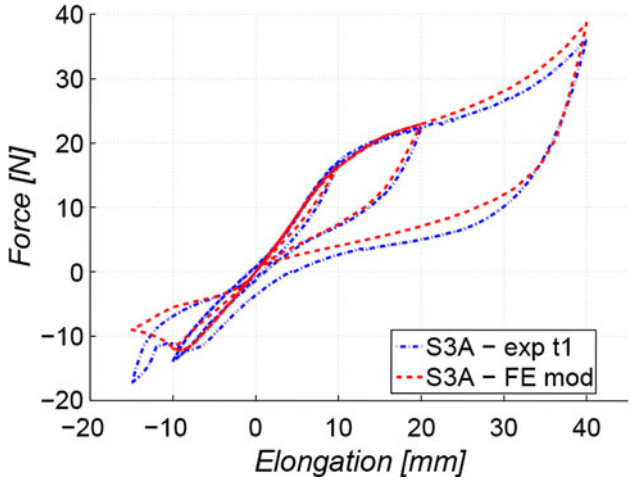

Fig. 15 Specimen S3A experimental and numerical test result comparison

5. Conclusions

In this study, summary of an investigation on the mechanical properties of a coil spring system has been reported. Coil spring is a classical device used in mechanics and characterized by well-defined theoretical design principles. Actually, they are used almost only in their elastic range. On the contrary, in this context superelastic spring response has been investigated through an experimental campaign. The superelastic spring is a recentering-theoretical zero residual displacement device. It provides a stable flag-shaped force-displacement response and large displacement capability with limited overall dimensions. Based on the experimental campaign results, coil spring system could be designed to be used as lateral restrain made of superelastic material. The field of application of such a flexible device type is very large. The main interest at the base of this study was related to civil engineering application as a lateral restraining system (see Ref 2, 3, 9), because the superelastic spring is characterized by a large displacement capability and nonlinear-recentering force. Nevertheless all the applications for which superelastic recentering effect and a relatively large displacement capability is attractive can take advantage of this device configuration.

A very simple numerical model has then been proposed and used to describe tested superelastic coil springs response and results are very good. There are some differences between the real response and the FE model results, but they can be considered negligible and the numerical analysis is able to predict all the main experimental data in terms of force-displacement relation. The most important discrepancies between numerical and experimental results are related to spring behavior in compression. A more accurate analysis campaign is proposed for future studies, taking into account the sensitivity of results to geometry imperfections. Nevertheless, due to its simplicity, the finite element model proposed in this study can be used to perform fast analyses and it is an important tool for pre-design springs which are supposed to reach a design maximum force and a design displacement.

A more comprehensive description on the experimental campaign on the numerical investigation and on the practical applications of the restraining system can be found in Ref 9.

References

1. A.M. Wahl, *Mechanical Springs*, Graw Hill, New York, 1963
2. G. Attanasi et al., Feasibility Assessment of An Innovative Isolation Bearing System With Shape Memory Alloys, *J. Earthq. Eng.*, 2009, **13**(1 (supp 1)), p 18–39
3. G. Attanasi and F. Auricchio, Innovative Superelastic Isolation Device, *J. Earthq. Eng.*, submitted for publication
4. G. Song, N. Ma, and H.-N. Li, Applications of Shape Memory Alloys in Civil Structures, *Eng. Struct.*, 2006, **28**, p 1266–1274
5. R. Desroches and B. Smith, Shape Memory Alloys in Seismic Resistant Design and Retrofit: A Critical Review of Their Potential and Limitations, *J. Earthq. Eng.*, 2003, **7**, p 1–15
6. J.C. Wilson and M.J. Wesolowsky, Shape Memory Alloys for Seismic Response Modification: A State-Of-The-Art Review, *Earthq. Spectra*, 2005, **21**(2), p 569–601
7. E.J. Graesser and F.A. Cozzarelli, Shape-Memory Alloys as New Materials for Aseismic Isolation, *J. Eng. Mech.*, 1991, **117**(11), p 2590–2608
8. ABAQUS, Analysis User's Manual Version 6.4., 2006, USA. Hibbitt, Karlsson & Sorensen Inc
9. G. Attanasi et al., "An Innovative Superelastic System For Base Isolation," PhD thesis, ROSE School, IUSS Pavia, August 2009